

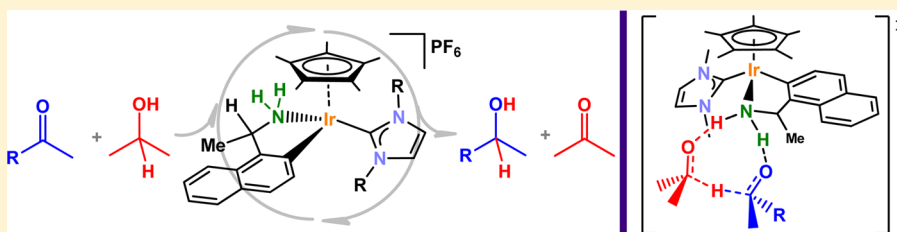
# Highly Active Cp\*Ir Catalyst at Low Temperatures Bearing an N-Heterocyclic Carbene Ligand and a Chelated Primary Benzylamine in Transfer Hydrogenation

Sara Sabater,<sup>†</sup> Miguel Baya,<sup>\*,‡</sup> and Jose A. Mata<sup>\*,†</sup>

<sup>†</sup>Departamento de Química Inorgánica y Orgánica, Universitat Jaume I, Avda. Sos Baynat s/n, 12071, Castellón, Spain

<sup>‡</sup>Instituto de Síntesis Química y Catálisis Homogénea (ISQCH), Departamento de Química Inorgánica, CSIC-Universidad de Zaragoza, C/Pedro Cerbuna 12, E-50009 Zaragoza, Spain

## Supporting Information



**ABSTRACT:** The synthesis of new Cp\*Ir complexes bearing an N-heterocyclic carbene ligand and a chelated primary benzylamine is described. The new complexes are chiral at metal and have a stereogenic carbon at the benzylamine ligand. The synthesis is diastereoselective, and the origin is thermodynamically controlled. The chiral complexes have been fully characterized. The catalytic results show that the complexes are very active in transfer hydrogenation: for example, acetophenone is reduced to 1-phenylethanol in 2 h at 50 °C using a catalyst loading of 1 mol %. More interestingly is that no base, apart from the required for catalyst activation, is needed in the process. The enantioselectivities obtained range from low to moderate, with a maximum of 58% ee in the case of 2'-methylacetophenone. Initial mechanistic studies by means of DFT calculations suggest that the mechanism is based on a direct hydrogen transfer via a highly ordered transition state centered at the iridium amido group. The calculations are in good agreement with the experimental data and support a concerted one-step mechanism process.

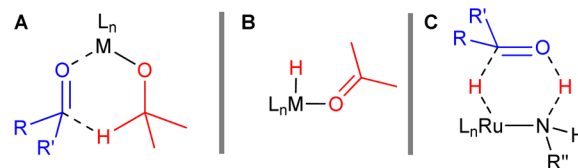
## INTRODUCTION

Transition-metal-catalyzed transfer hydrogenation (TH) is a well-established process for the reduction of carbonyls and imines under mild reaction conditions.<sup>1</sup> The asymmetric version gained considerable interest after the work developed by Noyori et al., who introduced chiral ruthenium complexes bearing primary amines that catalyze the transfer hydrogenation of ketones with iPrOH with high enantioselectivities.<sup>2</sup> Since then, many of the most effective catalysts involve the presence of primary or secondary amines as ligands.<sup>3</sup> The active catalytic species are formed after addition of a strong base to form the unsaturated metal-amido complexes.<sup>4</sup> From a mechanistic point of view, three main types of transfer hydrogenation pathways have been described either involving hydride derivatives or unsaturated metal species in the catalytic process. The *direct hydrogen transfer mechanism* (also known as Meerwein–Ponndorf–Verley, and Oppenauer for the reverse cycle) involves a six-membered transition state in which the metal acts as a Lewis acid and no participation of hydride intermediates is required.<sup>5</sup> The most common is the *migratory insertion mechanism*, which consists of an inner-sphere stepwise process that involves the insertion of the unsaturated bond into a metal hydride as a first step, followed by the proton transfer and elimination of the hydrogenated substrate.<sup>6</sup> The *concerted*

*hydrogen transfer mechanism* directly links with Noyori's bifunctional catalysts and proposes an outer-sphere process through a relatively ordered transition state, in which both a proton transfer and a hydride transfer to the unsaturated substrate happen with a certain degree of synchronicity.<sup>2c,k,m</sup> The key species proposed in these mechanisms are depicted in Chart 1.

Today a plethora of efficient transition-metal catalysts for TH based on Ru,<sup>7</sup> Rh,<sup>8</sup> and Ir<sup>9</sup> are known. Among them, the Cp\*Ir systems are emerging powerfully due to their stability and

**Chart 1. Key Species Proposed in the Mechanisms (A) Direct Hydrogen Transfer, (B) Migratory Insertion Inner Sphere, and (C) Concerted Hydrogen Transfer**



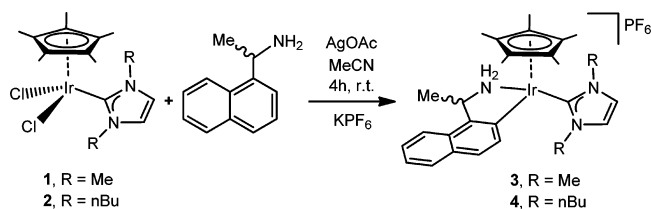
Received: August 29, 2014

activity,<sup>9d,10</sup> and even the first industrial application has recently been reported.<sup>11</sup> Encouraged by the catalytic abilities of Ir-NH type catalysts complexes developed by Ikariya<sup>12</sup> and Pfeffer,<sup>13</sup> and in light of our experience in metal catalysts based on N-heterocyclic carbene ligands we became interested in developing chiral Ir-NH catalysts with NHC ligands for transfer hydrogenation. In this work, we describe the synthesis of cationic highly active Cp\*Ir catalysts at low temperatures bearing an N-heterocyclic carbene ligand and a chelate primary benzylamine which we have used in transfer hydrogenation of prochiral ketones.<sup>14</sup> The Iridium complexes are chiral-at-metal and have a stereogenic carbon at the benzylamine ligand. Density functional theory studies have provided a mechanistic proposal which is consistent with the experimental observations and catalytic results. Interestingly, the transfer hydrogenation proceeds through a highly ordered transition state centered at the iridium amido group which does not properly fit into any of the three types of mechanisms discussed above.

## RESULTS AND DISCUSSION

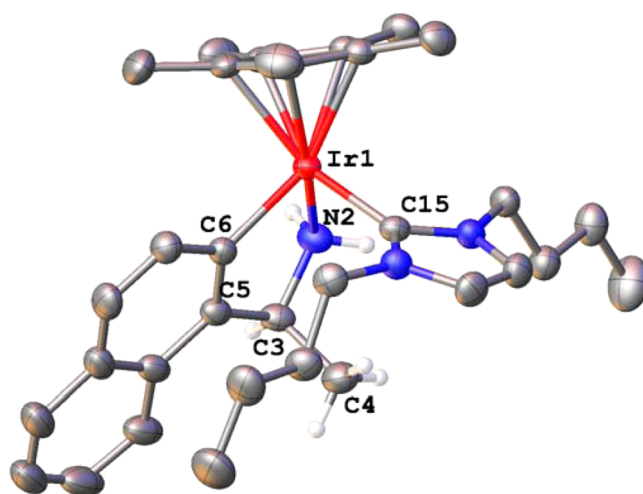
**Synthesis and Characterization of Racemic Catalysts. Transfer Hydrogenation of Ketones.** The reaction of [Cp\*Ir(Cl)<sub>2</sub>(Me<sub>2</sub>Im)] (1) or [Cp\*Ir(Cl)<sub>2</sub>(nBu<sub>2</sub>Im)] (2) with a racemic mixture of the primary amine [1-(1-naphthyl)ethyl]amine in the presence of 2 equiv of AgOAc affords the ortho-metalated iridium complexes 3 and 4, respectively (Scheme 1).

Scheme 1



Both complexes were obtained in high yields (92% and 85%, respectively) after being purified by column chromatography in silica gel. The cyclometalated iridium complexes are stable in an air atmosphere in the solid state and solution. The characterization of the complexes was made by means of NMR, high-resolution mass spectroscopy, and elemental analysis. The ortho-metalated nature of the compounds was initially confirmed by the data resulting from the electrospray mass spectrometry (ESI-MS) on the basis of the mass/charge relation and the isotopic pattern of peaks. Positive ion electrospray mass spectra analysis of complexes 3 and 4 in MeCN showed an intense peak for [M]<sup>+</sup> at *m/z* 594 and 678, respectively. High-resolution mass spectrometry (HRMS) confirmed the exact mass of these peaks with relative errors of less than 2 ppm. Direct evidence of cyclometalation is found in the <sup>1</sup>H NMR spectra. Complexes 3 and 4 show a doublet and a multiplet, respectively (7.96 ppm, d, *J* = 8.4 Hz, 1H, CH<sub>Ar</sub> for 3; 7.82–7.71 ppm, m, 2H, CH<sub>Ar</sub> for 4), assigned to the CH proton next to the ortho-metalated Ir–C bond.<sup>15</sup> The ortho-metalated complexes 3 and 4 are chiral at metal and have a stereogenic carbon; thus, in principle two diastereomers could be formed. The <sup>1</sup>H NMR and <sup>13</sup>C NMR spectra of complexes 3 and 4 show only one set of signals, indicating that only one diastereoisomer is formed (vide infra). The most characteristic signals in the <sup>13</sup>C NMR are those assigned to the metalated carbenes at δ 152.9 (complex 3) and 152.2 (complex 4).

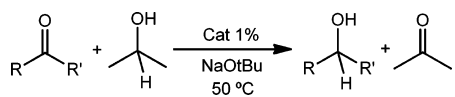
The molecular structure of complex 4 was confirmed by means of X-ray diffractometry (Figure 1). Single crystals were

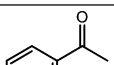
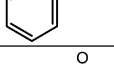
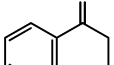
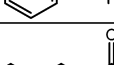
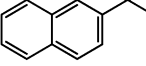
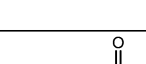
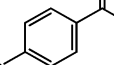
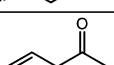
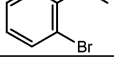
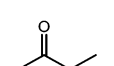
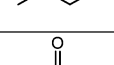
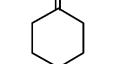


**Figure 1.** Molecular diagram of complex 4. Ellipsoids are given at the 50% probability level. Only hydrogen atoms bonded to N(2), C(3), and C(4) are shown. The counterion PF<sub>6</sub> has been omitted for clarity. Selected bond lengths (Å) and angles (deg): Ir(1)–C(15) 2.044(4), Ir(1)–N(2) 2.128(3), Ir(1)–C(6) 2.061(4), Ir(1)–Cp(cent) 1.861; C(6)–Ir(1)–N(2) 77.51(14), C(6)–Ir(1)–C(15) 94.34(15), C(15)–Ir(1)–N(2) 91.25(15).

obtained by slow evaporation of dichloromethane/hexane mixtures. Complex 4 crystallizes in the achiral space group *P* $\bar{1}$  and contains a single molecule in the asymmetric unit. This indicates that only one diastereoisomer is obtained as a pair of enantiomers, as confirmed previously by <sup>1</sup>H and <sup>13</sup>C NMR. The absolute configuration of the diastereoisomer shown in Figure 1 is *R<sub>Ir</sub>S<sub>C</sub>* according to the ligand priority sequence C<sub>5</sub>Me<sub>5</sub> > NH<sub>2</sub> > C<sub>carbene</sub> > Ph.<sup>16</sup> The geometry of the complex is the expected three-legged piano stool with dihedral angles close to 90° except for the C(6)–Ir(1)–N(2) angle of 77.51(14)° due to the chelate coordination of the [1-(1-naphthyl)ethyl]amine. The C–N ortho-metalated amine forms a five-membered ring in an envelope conformation, where the N atom is out of the plane by 0.34 Å. The methyl group C(4) attached at the benzylic carbon adopts an axial disposition enforced by the naphthyl group, as previously described for other complexes with this ligand.<sup>17</sup> The iridium distances are Ir(1)–C<sub>carbene</sub> 2.044(4) Å, Ir(1)–C(6) 2.061(4) Å, and Ir(1)–N(2) 2.128(3) Å and lie in the expected range for Cp\*Ir(NHC) complexes.

Complexes 3 and 4 were evaluated as catalyst precursors in transfer hydrogenation of ketones. Both complexes require the addition of a strong base to be active. The reactions were carried out using in *i*PrOH in the presence of catalytic amounts of *t*BuONa and a catalyst loading of 1 mol % (Table 1). Aromatic and aliphatic carbonyls are reduced to the corresponding alcohols in quantitative yields in 2 h at 70 °C, although most of the substrates only required 2 h at 50 °C to achieve yields over 95% (Table 1, entries 1–14). Acetophenone was converted into 1-phenylethanol quantitatively in 2 h at 50 °C using catalyst 3. When the same reaction was carried out using catalyst 4, only a 27% yield was obtained (entries 1 and 2). In all cases the catalyst activity of 3 is higher than that shown by catalyst 4 (entries 1–6), but for some substrates the difference is small even at 50 °C (entries 7–10). *p*-

Table 1. Transfer Hydrogenation using Complexes 3 and 4<sup>a</sup>


| Entry | Catalyst | Substrate   | Yield <sup>b</sup>   |
|-------|----------|---|----------------------|
| 1     | 3        |    | 100                  |
| 2     | 4        |    | 58(100) <sup>c</sup> |
| 3     | 3        |    | 95                   |
| 4     | 4        |    | 45(90) <sup>c</sup>  |
| 5     | 3        |    | 97                   |
| 6     | 4        |    | 55(100) <sup>c</sup> |
| 7     | 3        |    | 97                   |
| 8     | 4        |    | 92                   |
| 9     | 3        |    | 100                  |
| 10    | 4        |    | 97                   |
| 11    | 3        |   | 95                   |
| 10    | 4        |  | 57(100) <sup>c</sup> |
| 13    | 3        |  | 100                  |
| 14    | 4        |  | 100                  |

<sup>a</sup>Reactions were carried out with 0.5 mmol of substrate, *t*BuONa (5 mol %), catalyst (1 mol %), and 2 mL of 2-propanol for 2 h at 50 °C.

<sup>b</sup>Yields determined by GC analyses using anisole as internal standard.

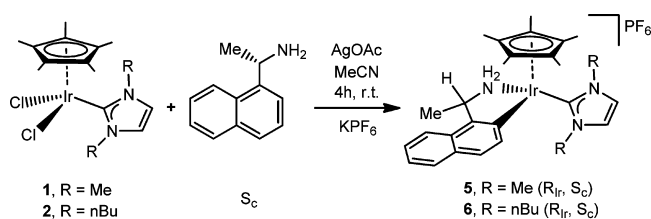
<sup>c</sup>Yields in parentheses after 2 h at 70 °C.

Bromoacetophenone is converted to the corresponding alcohol in short times and high yields using both catalysts (entries 7 and 8). No significant differences are observed for *o*-bromoacetophenone (entries 9 and 10).

### Synthesis and Characterization of Enantiomerically Pure Catalysts. Asymmetric Transfer Hydrogenation of Ketones.

Once we demonstrated the catalytic activity of the racemic complexes 3 and 4, we decided to prepare the chiral version of these catalysts. Following the same procedure described in Scheme 1, the reaction of [Cp\*Ir(Cl)<sub>2</sub>(Me<sub>2</sub>Im)] (1) or [Cp\*Ir(Cl)<sub>2</sub>(*n*Bu<sub>2</sub>Im)] (2) with the chiral primary amine (*S*)-[1-(1-naphthyl)ethyl]amine in the presence of 2 equiv of AgOAc affords the enantiopure iridium complexes 5 and 6 (Scheme 2). Complexes 5 and 6 were also obtained in high yields (92% and 85%, respectively) after being purified by

Scheme 2



column chromatography in silica gel. Characterization by ESI-MS and HRMS gave the same results as previously observed for complexes 3 and 4. The <sup>1</sup>H NMR and <sup>13</sup>C NMR spectra of complexes 5 and 6 show only one set of signals, indicating that only one diastereoisomer is formed. In both cases the isomer obtained is that where the methylene of the [1-(1-naphthyl)ethyl]amine is pointing away from the Cp\* ligand, as will be described below. The <sup>1</sup>H and <sup>13</sup>C NMR spectra of complex 5 are identical with those of 3. This is the first indication that the same diastereomer is obtained, although in this case there is just one enantiomer. The molecular structures of complexes 5 and 6 were obtained by X-ray crystallography and confirm the absolute configuration (*vide infra*). The circular dichroism (CD) spectrum of 5 shows three signals at λ 254, 281, and 327 nm for −10.2, 5.3, and 6.1 mdeg, respectively, and in the case of complex 3 no band is observed (Figure 2). The CD spectrum of 6 shows three signals at λ 251, 283, and 323 nm for −7.6, 2.6, and 3.5 mdeg, respectively, while complex 4 does not show any bands.

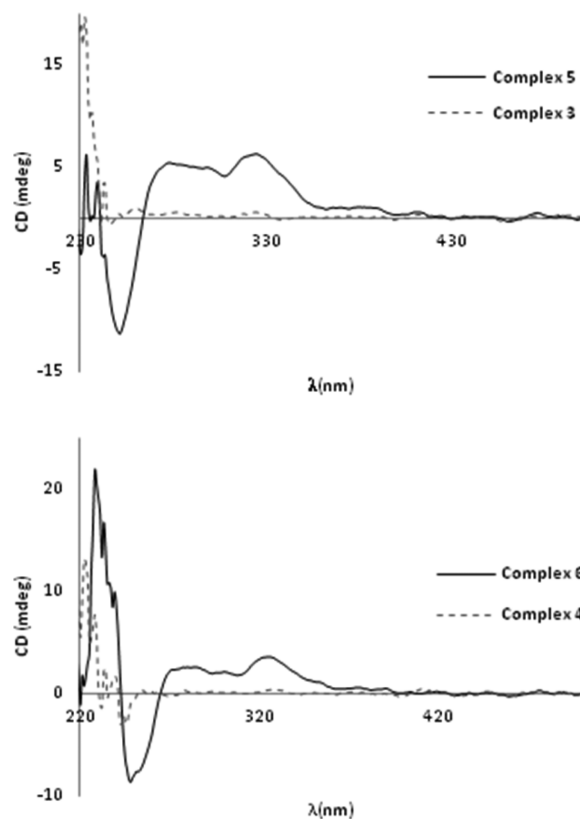


Figure 2. Circular dichroism spectra recorded in chloroform at 25 °C: (top) complex 3 (---) and complex 5 (—); (bottom) complex 4 (---) and complex 6 (—).

The molecular structure of complex 5 was confirmed by means of X-ray diffraction (Figure 3). Single crystals were obtained by slow evaporation of dichloromethane/hexane mixtures. Complex 5 crystallizes in the chiral space group *P*<sub>2</sub><sub>1</sub><sub>2</sub><sub>1</sub> and contains a single molecule in the asymmetric unit. This indicates that only one enantiomer is obtained. The absolute configuration of the enantiomer shown in Figure 3 is R<sub>f</sub>S<sub>c</sub> according to the ligand priority sequence C<sub>5</sub>Me<sub>5</sub> > NH<sub>2</sub> > C<sub>carbene</sub> > Ph. The geometry of complex 5 and bond lengths and angles are similar to those described for complex 4 (Figure 1).



derived from the presence of different conformers. The transfer hydrogenation reaction was studied using isopropyl alcohol and acetophenone as hydrogen source and hydrogen acceptor, respectively, as model substrates.<sup>9c,18</sup>

The experimental results show that the iridium(III) catalytic systems obtained in this work are highly active in the transfer hydrogenation process at low temperatures. The reaction proceeds at relatively low temperatures (30 °C), and the ee values obtained ranged from low to moderate. Other points that deserve further discussion are the following. (i) We have not observed decoordination of any of the ligands in the metal coordination sphere during the course of the experimental studies, although very recently catalyst activation by loss of Cp\* has been reported in Cp\*Ir complexes bearing two NHCs.<sup>10b</sup> (ii) We did not find any evidence supporting either the formation of a hydride complex or the participation of a such type of species in the catalytic cycle. These and the imperative need for a strong base in the reaction media to activate the catalyst (5:1 base to catalyst molar ratio) suggest an outer-sphere mechanism involving an iridium amido derivative as the active species in the catalytic cycle, with the iridium amine precursor remaining as the resting state.

Whereas important efforts have been devoted to the determination of the mechanisms operating in Ru-catalyzed TH reactions by means of theoretical calculations,<sup>10d,18b,19</sup> analogous studies on TH processes promoted by iridium systems are scarce.<sup>7b,9c,20</sup> As a starting point, the relative energies of the two pairs of enantiomers were evaluated. The  $R_{Ir}S_C/S_{Ir}R_C$  pair (**5a-DFT**) is found to be 1.6 kcal/mol more stable ( $\Delta G_{\text{PrOH}}$ ) than the  $R_{Ir}R_C/S_{Ir}S_C$  pair (**5b-DFT**) (Scheme S1, Supporting Information). Although small barriers have to be taken with caution, this relative energy order is in agreement with the experimental results found in the synthesis of complexes **3** and **4** (Scheme 1), suggesting that the process is thermodynamically controlled. The converged structure of **5a-DFT** compares well with that found for **5** by X-ray crystallography, with the five-member aza-irida-metallacycle ring showing an envelope conformation in which the N atom is slightly out of the plane, by 0.46 Å. The Ir–C<sub>carbene</sub>, Ir–C<sub>metallacycle</sub>, and Ir–N bond distances in **5a-DFT** are 2.06, 2.08, and 2.19 Å, respectively.

A second issue that has been addressed is the interaction of the base with the catalyst precursor. Both the interaction of the alkoxide with any of the two hydrogen NH atoms and the formation of an iridium alkoxide complex via amine decoordination have been considered. The three most remarkable adducts found are shown in Figure 5 and their relative energies in Scheme 3. The most favored alkoxide species (**A-DFT**) lies 22.5 kcal/mol higher in free energy in solution with regard to the most favored amido alcohol species (**B-DFT**) and 17.9 kcal/mol higher than a second amido alcohol isomer (**C-DFT**). These relative energies highlight the unlikelihood of the participation of an iridium alkoxide species in the cycle.

The structure of the putative iridium amido complex resulting from the deprotonation of **5** was optimized (**D-DFT**; Figure 5). This species is most likely the catalyst of the studied TH process, as pointed out by the experimental and theoretical evidence. Two mechanisms consistent with the discussion presented above have been considered. The first one (pathway 1-P1, Scheme 4) can be described as a *concerted, two-step, outer-sphere process*, involving the participation of the cyclopentadienyl ring and the amido group.<sup>21</sup> In the first step,

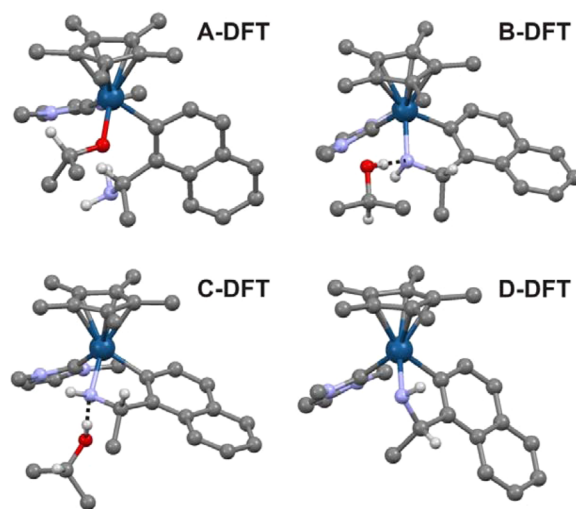
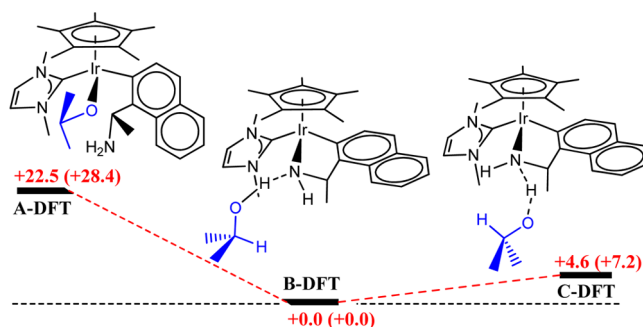


**Figure 5.** Molecular diagrams of the DFT optimized complexes and adducts **A-DFT**, **B-DFT**, **C-DFT**, and **D-DFT**. Most hydrogen atoms have been omitted for clarity.

**Scheme 3. Relative Free Energies in Solution (<sup>i</sup>PrOH) of the Iridium Alkoxide (**A-DFT**) and Amido Alcohol Species (**B-DFT** and **C-DFT**)<sup>a</sup>**



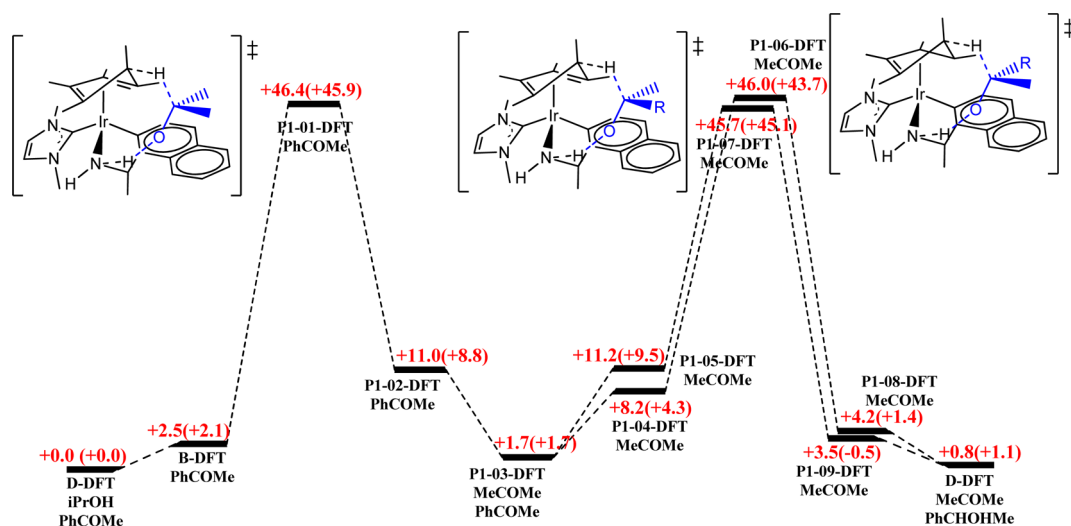
<sup>a</sup>Relative free energies in the gas phase are shown in parentheses.

the iridium amido complex **D-DFT** would dehydrogenate isopropyl alcohol to give an iridium amine  $\eta^4$ -cyclopentadiene species (**P1-3-DFT**) that would subsequently transfer H<sub>2</sub> to the prochiral ketone in the second step (Scheme 4). This latter transfer could happen with two possible substrate orientations, thus leading to the formation of the two alcohol enantiomers (*R* and *S*).

The key species of this depicted cycle is the iridium amine  $\eta^4$ -cyclopentadiene **P1-3-DFT**, which would result from the alcohol to catalyst transfer hydrogenation. Notably, the calculated transition state for the first step (**P1-1-DFT**) is 46.6 kcal/mol higher in  $\Delta G(\text{PrOH})$  value with regard to the free reactants. Consistent with this barrier, the subsequent transfer hydrogenations from **P1-3-DFT** to the prochiral ketone in any of the two possible orientations, therefore rendering (*S*)- or (*R*)-1-phenylethanol, also require 46.0 and 45.7 kcal/mol, respectively (transition states **P1-6-DFT** and **P1-7-DFT**). Thus, the high energy barriers calculated for these processes (dehydrogenation–transfer hydrogenation) clearly dismiss this reaction pathway.

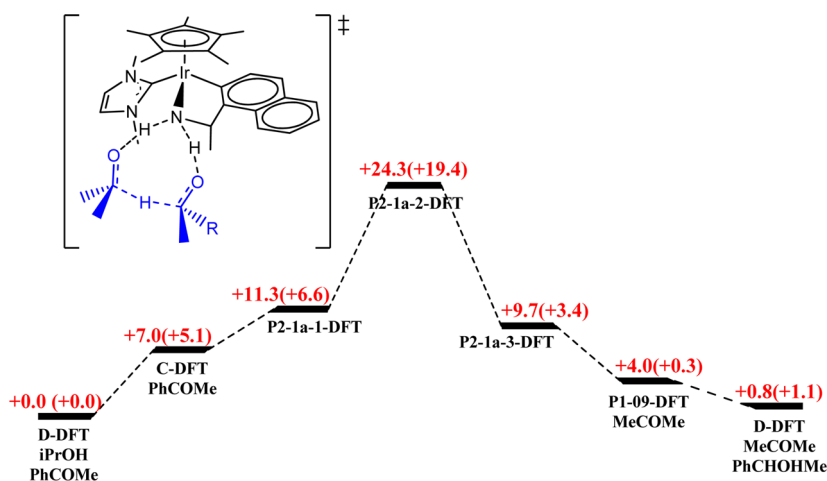
The second mechanism would consist of the transfer hydrogenation from the iridium amido–isopropyl alcohol adduct (either **B-DFT** or **C-DFT**, see above) to the prochiral ketone, in a *concerted, one-step, outer-sphere process*. Thus,

Scheme 4. DFT-Calculated Energy Profile for the Concerted, Two-Step, Outer-Sphere Hydrogen Transfer Mechanism (Pathway 1)<sup>a</sup>



<sup>a</sup>Relative free energies in <sup>i</sup>PrOH solution and in the gas phase (in parentheses) are shown. Only TSs are shown for clarity.

Scheme 5. DFT-Calculated Energy Profile for One of the Four Possible Concerted, One-Step, Outer-Sphere Hydrogen Mechanisms (Pathway 2-1a)<sup>a</sup>



<sup>a</sup>Relative free energies in <sup>i</sup>PrOH solution and in the gas phase (in parentheses) are shown. Only the TS is shown for clarity.

depending on the relative orientation of the alcohol and the prochiral ketone with regard to the iridium catalyst, four variants can be envisaged, alternatively leading to the formation of one of the two enantiomers. For clarity, only one of these pathways is shown in the main text (Scheme 5). The complete series, including the four different variants of the mechanism and the species involved, can be found in the Supporting Information (Scheme S2-5).

Four different transition states were found (Figure 6), two of them leading to (*R*)-1-phenylethanol (P2-1a-2-DFT, P2-2b-2-DFT), and the other two leading to (*S*)-1-phenylethanol (P2-1b-2-DFT, P2-2a-2-DFT). Interestingly, the calculated energy barriers ( $\Delta G_{\text{solv}}$ ) of these concerted processes lay in the 24.3–25.7 kcal/mol range (18.6–21.2 kcal/mol in  $\Delta G_{\text{gas}}$ ), data that seem consistent with the experimental results. Furthermore, the relative energies of the TSs found leading to either the *R* or the *S* alcohol enantiomers present very similar values with regard to each other. In other words, the DFT calculations do not predict remarkable ee values in favor of any of the enantiomers. This

result also seems in good agreement with the poor enantiomeric excess obtained in the studied experiment.

The whole set of transition states found for this mechanism are “hydrogen-bonding organized” TSs. All of them are markedly synchronous, thus supporting concerted processes. The most significant geometric parameters are collected in Table 3. The H...O distances in the referred transition states only vary from 1.77 to 1.93 Å (distances c and d), whereas the H...C distances remain in the 1.33–1.39 Å range (distances g and h). Hydrogen bonding organized transition states have been proposed previously in a few catalytic reactions, including the Ru-catalyzed enantioselective Michael addition of 1,3-dicarbonyl compounds to cyclic enones and the Ir-catalyzed asymmetric transfer hydrogenation of nitroalkenes.<sup>20b,22</sup>

In order to gain additional experimental evidence for the proposed mechanism, replacement of the NH group by an N-alkyl group was investigated. The introduction of this alkyl group should inhibit the formation of the hydrogen bonding organized transition state and have an effect on the catalytic

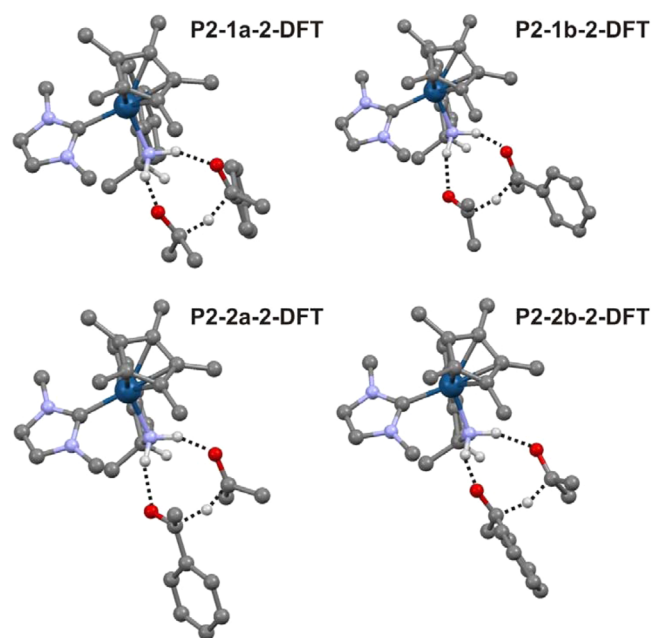


**Figure 6.** Molecular diagrams of the DFT optimized transition states P2-1a-2-DFT, P2-1b-2-DFT, P2-2a-2-DFT, and P2-2b-2-DFT. Most hydrogen atoms have been omitted for clarity.

activity. The reaction of  $[\text{Cp}^*\text{Ir}(\text{Cl})_2(\text{Me}_2\text{Im})]$  (**1**) or  $[\text{Cp}^*\text{Ir}(\text{Cl})_2(\text{nBu}_2\text{Im})]$  (**2**) with the secondary amine (*S*)-*N*, $\alpha$ -dimethylbenzylamine in the presence of 2 equiv of AgOAc under the same conditions as described in Scheme 1 did not afford any ortho-metalated complex. Modifying the reaction conditions by increasing the temperature gave the same result.

It is well-known that NH moieties of ligands have unique functions that can give rise to wide applications in organometallic catalysis.<sup>3</sup> These include the recognition and/or

activation of certain substrates, which can afford improved catalytic activities and/or selectivities. The catalysts presented in this work also constitute a rare and remarkable example showing that inert, octahedral, chiral at metal complexes can have successful applications in catalysis. Thus, despite the inertness toward substitution reactions of our  $\text{Cp}^*\text{Ir}(\text{III})$  systems, transfer hydrogenation processes efficiently proceed mediated by the NH ligand. Substitutionally inert species, if catalytically active, may lead to robust catalysts, therefore presenting higher turnover numbers. Although up to now our complexes only induce low to moderate ee values, the synergy among  $\text{Cp}^*\text{Ir}$  moieties, NHC ligands, and primary amines holds great promise for the design of bulky systems showing improved performances in asymmetric transfer hydrogenations, and also in other catalytic processes. Further studies are currently underway in our laboratory and will be reported in due course.

## CONCLUSIONS

We have described the synthesis on new  $\text{Cp}^*\text{Ir}$  complexes bearing an N-heterocyclic carbene ligand and a chelated primary benzylamine. The complexes are chiral at metal and have a stereogenic carbon at the benzylamine ligand. The synthesis is diastereoselective, and the origin is thermodynamically controlled. From the catalytic results, we conclude that cyclometalated iridium complexes based on chiral primary benzylamines are very active in transfer hydrogenation: for example, acetophenone is reduced to 1-phenylethanol in 2 h at 50 °C using catalyst **3**. More interestingly is that no base, apart from that required for catalyst activation, is needed in the process. Unfortunately, the enantioselectivities obtained using the chiral benzylamines are from low to moderate, achieving a maximum of 58% ee in the case of 2'-methylacetophenone. Preliminary mechanistic studies by means of DFT calculations suggest that the mechanism is based on a direct hydrogen

**Table 3.** Relative Energies and Representative Geometric Parameters of the Four Transition States Found for the Concerted, One-Step, Outer-Sphere Hydrogen Mechanism (Pathway 2)<sup>a</sup>

| distance                 | P2-1a-2-DFT (R1a = Ph) | P2-1b-2-DFT (R1b = Ph) | P2-2a-2-DFT (R2a = Ph) | P2-2b-2-DFT (R2b = Ph) |
|--------------------------|------------------------|------------------------|------------------------|------------------------|
| enantiomer               | R                      | S                      | S                      | R                      |
| $\Delta G(\text{iPrOH})$ | 24.3                   | 24.6                   | 24.7                   | 25.7                   |
| $\Delta G(\text{gas})$   | 19.4                   | 18.6                   | 18.8                   | 21.2                   |
| N–H                      | a                      | 1.04                   | 1.04                   | 1.04                   |
| N–H                      | b                      | 1.04                   | 1.04                   | 1.04                   |
| H...O                    | c                      | 1.85                   | 1.81                   | 1.79                   |
| H...O                    | d                      | 1.77                   | 1.89                   | 1.93                   |
| O=C                      | e                      | 1.27                   | 1.28                   | 1.29                   |
| O=C                      | f                      | 1.28                   | 1.28                   | 1.28                   |
| C...H                    | g                      | 1.39                   | 1.33                   | 1.33                   |
| C...H                    | h                      | 1.34                   | 1.35                   | 1.36                   |

<sup>a</sup>Energies are expressed in kcal/mol and distances in Å.

transfer via highly ordered transition state centered at the iridium amido group. An understanding of the mechanism will allow the rational design of new and more efficient catalysts for asymmetric hydrogen transfer. Further mechanistic investigations and the preparation of Cp\*Ir complexes with different chiral primary amines are currently underway in our laboratory.

## EXPERIMENTAL SECTION

**General Procedures.** All manipulations were carried out under nitrogen using standard Schlenk techniques and high vacuum, unless otherwise stated. Compounds **1** and **2** were prepared according to literature procedures. Anhydrous solvents were dried using a solvent purification system or were purchased from commercial suppliers and degassed prior to use by purging with dry nitrogen and kept over molecular sieves. NMR spectra were recorded on Varian Innova spectrometers operating at 300 or 500 MHz (<sup>1</sup>H NMR) and 75 and 125 MHz (<sup>13</sup>C NMR), respectively, using CDCl<sub>3</sub> as solvent at room temperature unless otherwise stated. Elemental analyses were carried out in an EA 1108 CHNS-O Carlo Erba analyzer. Electrospray mass spectra (ESI-MS) were recorded on a MicromassQuattro LC instrument, and nitrogen was employed as drying and nebulizing gas. Circular dichroism (CD) measurements were recorded on a JASCO J-810 spectropolarimeter in chloroform solutions.

**X-ray Studies.** Diffraction data were collected on a Agilent SuperNova diffractometer equipped with an Atlas CCD detector using Mo K $\alpha$  radiation ( $\lambda = 0.71073$  Å). Single crystals were mounted on a polymer tip in a random orientation. Absorption corrections based on the multiscan method were applied.<sup>23</sup> The structures were solved by direct methods in SHELXS-97 and refined by the full-matrix method based on  $F^2$  with the program SHELXL-97 using the OLEX software package.<sup>24</sup> CCDC-1010664 (**4**), CCDC-1010665 (**5**), and CCDC-1010666 (**6**) contain the supplementary crystallographic data for this paper. These data can be obtained free of charge from The Cambridge Crystallographic Data Centre via [www.ccdc.cam.ac.uk/data\\_request/cif](http://www.ccdc.cam.ac.uk/data_request/cif).

**Computational Details.** Quantum mechanical calculations were performed with the Gaussian09 package<sup>25</sup> at the DFT/M06 level of theory.<sup>26</sup> The SDD basis set and its corresponding effective core potentials (ECPs) were used to describe the iridium atom.<sup>27</sup> An additional set of *f*-type functions was also added.<sup>28</sup> Carbon, nitrogen, oxygen, and hydrogen atoms were described with a 6-31G\*\* basis set.<sup>29,30</sup> Frequency calculations have been performed in order to determine the nature of the stationary points found (no imaginary frequencies for minima, only one imaginary frequency for transition states). Free Gibbs energies in <sup>1</sup>PrOH solution ( $\epsilon = 19.264$ ) were calculated by computing the energy in the solvent by means of single-point calculations on the gas-phase optimized geometries with the SMD continuum solvation model,<sup>31</sup> and subsequently applying the expression

$$G_{\text{IrPrOH}} = E_{\text{IrPrOH}} + (G_{\text{gas phase}} - E_{\text{gas phase}})$$

The TS's connecting two minima were investigated by using a freeze-scan strategy. C...H distances involved in the C–H bond forming processes have been frozen in subsequent 0.05 Å steps, and the structures have been optimized with the referred restriction. The optimized geometry for the first point has been used as a starting one for the following point in the profile, and the process has been repeated for subsequent points. A first approximation for the C–H...C to C...H–C reaction energy profile is therefore obtained. The highest energy structure in each studied profile is then used as a starting geometry in order to find the corresponding TS. In all cases the shape of the transition vector provided by the frequency calculation in each of the TS's is consistent with the proposed mechanism. IRC computations have been additionally carried out in order to connect minima and TSs and further strengthen the mechanism proposal. Three-dimensional visualization of all the optimized structures discussed is accessible as Supporting Information.

**Synthesis of Compounds 3 and 4.** In a Schlenk flask were placed 0.17 mmol of the corresponding iridium compound (**1** or **2**), 0.34 mmol of silver acetate, and 10 mL of deoxygenated acetonitrile. The mixture was stirred at room temperature for 15 min. To the suspension was added 0.17 mmol of 1-(1-naphthyl)ethylamine, and the mixture was stirred at room temperature for 4 h. The resulting mixture was filtered over Celite, and the solvent was removed under reduced pressure. The crude product was purified by column chromatography. Elution with acetone–KPF<sub>6</sub> solution afforded the separation of a yellow band that contained the title compound. Crystallization from dichloromethane/hexane gave the corresponding compound as a yellow crystalline solid.

**Compound 3.** Yield: 117 mg (92%). <sup>1</sup>H NMR (300 MHz, CD<sub>3</sub>CN):  $\delta$  7.96 (d, *J* = 8.4 Hz, 1H, CH<sub>Ar</sub>), 7.80 (d, *J* = 8.5 Hz, 1H, CH<sub>Ar</sub>), 7.65–7.53 (m, 2H, CH<sub>Ar</sub>), 7.41–7.27 (m, 2H, CH<sub>Ar</sub>), 7.19 (d, *J* = 1.9 Hz, 1H, CH<sub>imidazole</sub>), 6.97 (d, *J* = 1.9 Hz, 1H, CH<sub>imidazole</sub>), 5.07 (broad s, 1H, NH<sub>2</sub>), 5.01–4.87 (m, 1H, CHCH<sub>3</sub>), 3.90 (s, 3H, NCH<sub>3</sub>), 3.80 (broad s, 1H, NH<sub>2</sub>), 3.32 (s, 3H, NCH<sub>3</sub>), 1.72 (s, 15H, C<sub>5</sub>(CH<sub>3</sub>)<sub>5</sub>), 0.66 (d, *J* = 6.8 Hz, 3H, CHCH<sub>3</sub>). <sup>13</sup>C{<sup>1</sup>H} NMR (75 MHz, CD<sub>3</sub>CN):  $\delta$  152.9 (C<sub>carbene</sub>-Ir), [148.2, 142.6, 138.8, 131.8, 129.1, 128.7, 126.7, 126.1, 125.5, 124.2 (C<sub>Ar</sub>)], [123.9, 123.8 (CH<sub>imidazole</sub>)], 92.2 (C<sub>5</sub>(CH<sub>3</sub>)<sub>5</sub>), 59.3 (CHCH<sub>3</sub>), [39.2, 39.0 (NCH<sub>3</sub>)], 18.9 (CHCH<sub>3</sub>), 9.2 (C<sub>5</sub>(CH<sub>3</sub>)<sub>5</sub>). Anal. Calcd for C<sub>27</sub>H<sub>35</sub>N<sub>3</sub>IrPF<sub>6</sub> (738.77): C, 43.89; H, 4.77; N, 5.68. Found: C, 44.25; H, 4.26; N, 5.74. Electrospray MS (cone 20 V; *m/z*, fragment): 594.2 [M]<sup>+</sup>. HRMS ESI-TOF-MS (positive mode): [M]<sup>+</sup> monoisotopic peak 594.2464; calcd 594.2462,  $\epsilon_r$  0.3 ppm.

**Compound 4.** Yield: 120 mg (85%). <sup>1</sup>H NMR (300 MHz, CD<sub>2</sub>Cl<sub>2</sub>):  $\delta$  7.82–7.71 (m, 2H, CH<sub>Ar</sub>), 7.61–7.48 (m, 2H, CH<sub>Ar</sub>), 7.39–7.23 (m, 2H, CH<sub>Ar</sub>), 7.17 (d, *J* = 2.1 Hz, 1H, CH<sub>imidazole</sub>), 6.93 (d, *J* = 2.1 Hz, 1H, CH<sub>imidazole</sub>), 5.06–4.91 (m, 1H, CHCH<sub>3</sub>), 4.72 (broad s, 1H, NH<sub>2</sub>), 4.30–4.13 (m, 1H, NCH<sub>2</sub>-), 4.13–3.94 (m, 2H, NCH<sub>2</sub>-), 3.85 (broad s, 1H, NH<sub>2</sub>), 3.71–3.55 (m, 1H, NCH<sub>2</sub>-), 2.16–1.98 (m, 1H, –CH<sub>2</sub>-), 1.98–1.79 (m, 1H, –CH<sub>2</sub>-), 1.74–1.58 (m, 17H, C<sub>5</sub>(CH<sub>3</sub>)<sub>5</sub>, –CH<sub>2</sub>-), 1.14–0.98 (m, 7H, –CH<sub>2</sub>-, –CH<sub>3</sub>), 0.66 (d, *J* = 6.8 Hz, 3H, CHCH<sub>3</sub>), 0.58 (t, *J* = 7.1 Hz, 3H, –CH<sub>3</sub>). <sup>13</sup>C{<sup>1</sup>H} NMR (75 MHz, CD<sub>3</sub>CN):  $\delta$  152.2 (C<sub>carbene</sub>-Ir), [148.1, 142.7, 137.9, 131.7, 129.1, 128.4, 127.0, 126.8, 124.3 (C<sub>Ar</sub>)], [123.9, 123.7 8 (CH<sub>imidazole</sub>)], 122.0 (C<sub>Ar</sub>), 92.3 (C<sub>5</sub>(CH<sub>3</sub>)<sub>5</sub>), 59.5 (CHCH<sub>3</sub>), [51.5, 50.4 (N–CH<sub>2</sub> *n*-Bu)], [33.6, 33.5 (–CH<sub>2</sub>–CH<sub>2</sub> *n*-Bu)], [21.0, 20.4 (–CH<sub>2</sub>–CH<sub>3</sub> *n*-Bu)], 19.3 (CHCH<sub>3</sub>), [14.2, 13.8 (–CH<sub>3</sub> *n*-Bu)], 9.2 (C<sub>5</sub>(CH<sub>3</sub>)<sub>5</sub>). Anal. Calcd for C<sub>33</sub>H<sub>47</sub>N<sub>3</sub>IrPF<sub>6</sub> (822.93): C, 48.16; H, 5.75; N, 5.10. Found: C, 48.46; H, 5.97; N, 5.33. Electrospray MS (cone 20 V; *m/z*, fragment): 678.5 [M]<sup>+</sup>. HRMS ESI-TOF-MS (positive mode): [M]<sup>+</sup> monoisotopic peak 678.3411; calcd 678.3401,  $\epsilon_r$  1.5 ppm.

**Synthesis of Compounds 5 and 6.** In a Schlenk flask were placed 0.17 mmol of the corresponding iridium compound and 0.34 mmol of silver acetate, and 10 mL of deoxygenated acetonitrile was added. The mixture was stirred at room temperature for 15 min. To the suspension was added 0.172 mmol of (S)-(–)-1-(1-naphthyl)ethylamine, and the mixture was stirred at room temperature for 4 h. The resulting mixture was filtered over Celite, and the solvent was removed under reduced pressure. The crude product was purified by column chromatography. Elution with acetone–KPF<sub>6</sub> solution afforded the separation of a yellow band that contained the compound and residual KPF<sub>6</sub>, which was filtered off. Crystallization from dichloromethane/hexane gave the corresponding compound as a yellow crystalline solid.

**Compound 5.** Yield: 102 mg (80%). <sup>1</sup>H NMR (300 MHz, CD<sub>3</sub>CN):  $\delta$  7.96 (d, *J* = 8.3 Hz, 1H, CH<sub>Ar</sub>), 7.80 (d, *J* = 7.6 Hz, 1H, CH<sub>Ar</sub>), 7.65–7.53 (m, 2H, CH<sub>Ar</sub>), 7.42–7.24 (m, 2H, CH<sub>Ar</sub>), 7.19 (d, *J* = 1.9 Hz, 1H, CH<sub>imidazole</sub>), 6.97 (d, *J* = 1.9 Hz, 1H, CH<sub>imidazole</sub>), 5.07 (broad s, 1H, NH<sub>2</sub>), 5.01–4.89 (m, 1H, CHCH<sub>3</sub>), 3.90 (s, 3H, NCH<sub>3</sub>), 3.80 (broad s, 1H, NH<sub>2</sub>), 3.32 (s, 3H, NCH<sub>3</sub>), 1.73 (s, 15H, C<sub>5</sub>(CH<sub>3</sub>)<sub>5</sub>), 0.66 (d, *J* = 6.6 Hz, 3H, CHCH<sub>3</sub>). <sup>13</sup>C{<sup>1</sup>H} NMR (75 MHz, CD<sub>3</sub>CN):  $\delta$  152.9 (C<sub>carbene</sub>-Ir), [148.2, 142.6, 138.8, 131.8, 129.1, 128.7, 126.7, 126.1, 125.5, 124.2 (C<sub>Ar</sub>)], [123.9, 123.8 (CH<sub>imidazole</sub>)], 92.2 (C<sub>5</sub>(CH<sub>3</sub>)<sub>5</sub>), 59.3 (CHCH<sub>3</sub>), [39.2, 39.0 (NCH<sub>3</sub>)], 18.9 (CHCH<sub>3</sub>), 9.2 (C<sub>5</sub>(CH<sub>3</sub>)<sub>5</sub>). Anal. Calcd for C<sub>27</sub>H<sub>35</sub>N<sub>3</sub>IrPF<sub>6</sub>

(738.77): C, 43.89; H, 4.77; N, 5.68. Found: C, 44.36; H, 4.61; N, 5.80. Electrospray MS (cone 20 V;  $m/z$ , fragment): 594.2  $[M]^+$ . HRMS ESI-TOF-MS (positive mode):  $[M]^+$  monoisotopic peak 594.2465; calcd 594.2462,  $\epsilon_r$  0.4 ppm.

**Compound 6.** Yield: 133 mg (94%).  $^1\text{H}$  NMR (300 MHz,  $\text{CD}_2\text{Cl}_2$ ):  $\delta$  7.82–7.71 (m, 2H,  $\text{CH}_{\text{Ar}}$ ), 7.61–7.48 (m, 2H,  $\text{CH}_{\text{Ar}}$ ), 7.39–7.23 (m, 2H,  $\text{CH}_{\text{Ar}}$ ), 7.17 (d,  $J = 2.1$  Hz, 1H,  $\text{CH}_{\text{imidazole}}$ ), 6.93 (d,  $J = 2.1$  Hz, 1H,  $\text{CH}_{\text{imidazole}}$ ), 5.06–4.91 (m, 1H,  $\text{CHCH}_3$ ), 4.72 (broad s, 1H,  $\text{NH}_2$ ), 4.30–4.13 (m, 1H,  $\text{NCH}_2$ ), 4.13–3.94 (m, 2H,  $\text{NCH}_2$ ), 3.85 (broad s, 1H,  $\text{NH}_2$ ), 3.71–3.55 (m, 1H,  $\text{NCH}_2$ ), 2.16–1.98 (m, 1H,  $-\text{CH}_2-$ ), 1.98–1.79 (m, 1H,  $-\text{CH}_2-$ ), 1.74–1.58 (m, 17H,  $\text{C}_5(\text{CH}_3)_5$ ,  $-\text{CH}_2-$ ), 1.14–0.98 (m, 7H,  $-\text{CH}_2-$ ,  $-\text{CH}_3$ ), 0.66 (d,  $J = 6.8$  Hz, 3H,  $\text{CHCH}_3$ ), 0.58 (t,  $J = 7.1$  Hz, 3H,  $-\text{CH}_3$ ).  $^{13}\text{C}\{^1\text{H}\}$  NMR (75 MHz,  $\text{CD}_3\text{CN}$ ):  $\delta$  152.2 ( $\text{C}_{\text{carbene-Ir}}$ ), [148.1, 142.7, 137.9, 131.7, 129.1, 128.4, 127.0, 126.8, 124.3 ( $\text{C}_{\text{Ar}}$ )], [123.9, 123.7 8 ( $\text{CH}_{\text{imidazole}}$ )], 122.0 ( $\text{C}_{\text{Ar}}$ ), 92.3 ( $\text{C}_5(\text{CH}_3)_5$ ), 59.5 ( $\text{CHCH}_3$ ), [51.5, 50.4 ( $\text{N}-\text{CH}_2$ -  $n$ -Bu)], [33.6, 33.5 ( $-\text{CH}_2-\text{CH}_2$   $n$ -Bu)], [21.0, 20.4 ( $-\text{CH}_2-\text{CH}_3$   $n$ -Bu)], 19.3 ( $\text{CHCH}_3$ ), [14.2, 13.8 ( $-\text{CH}_3$   $n$ -Bu)], 9.2 ( $\text{C}_5(\text{CH}_3)_5$ ). Anal. Calcd for  $\text{C}_{33}\text{H}_{47}\text{N}_3\text{IrPF}_6\cdot 3\text{C}_6\text{H}_{14}$  (1081.45): C, 56.64; H, 8.29; N, 3.88. Found: C, 56.21; H, 8.31; N, 3.96. Electrospray MS (cone 20 V) ( $m/z$ , fragment): 678.3  $[M]^+$ . HRMS ESI-TOF-MS (positive mode):  $[M]^+$  monoisotopic peak 678.3412; calcd 678.3401,  $\epsilon_r$  1.6 ppm.

**Catalytic Studies. General Procedure for Transfer Hydrogenation.** The iridium complex (1 mol %) and  $t\text{BuONa}$  (5 mol %) were placed together in a Schlenk tube with a Teflon cap. The tube was then evacuated and filled with nitrogen three times. 2-Propanol (2 mL) and the corresponding ketone (0.5 mmol) were added, and the mixture was stirred at 50 °C for 2 h. Yields were determined by GC analyses using anisole (0.5 mmol) as internal standard.

**General Procedure for Asymmetric Transfer Hydrogenation.** The iridium complex (1 mol %) and  $t\text{BuONa}$  (5 mol %) were placed together in a Schlenk tube with a Teflon cap. The tube was then evacuated and filled with nitrogen three times. 2-Propanol (2 mL) and the corresponding ketone (0.5 mmol) were added, and the mixture was stirred at 30 °C for 8 h. Yields were determined by GC analyses using anisole (0.5 mmol) as internal standard. The ee was determined using chiral GC.

## ■ ASSOCIATED CONTENT

### ● Supporting Information

Text, tables, figures, CIF files giving details of the catalytic experiments, high-resolution mass spectra (HR/MS), nuclear magnetic resonance (NMR), circular dichroism, X-ray diffraction data, complete ref 25, and computed Cartesian coordinates of all of the molecules reported in this study. This material is available free of charge via the Internet at <http://pubs.acs.org>.

## ■ AUTHOR INFORMATION

### Corresponding Authors

\*M.B.: e-mail, [mbaya@unizar.es](mailto:mbaya@unizar.es); fax, (+34) 976761187; tel, (+34) 976761184.

\*J.A.M.: e-mail, [jmata@uji.es](mailto:jmata@uji.es); tel, (+34) 964387516; fax, (+34) 964387522.

### Notes

The authors declare no competing financial interest.

## ■ ACKNOWLEDGMENTS

We acknowledge financial support from the Ministerio de Ciencia e Innovación of Spain (CTQ2011-24055/BQU) and the Gobierno de Aragón (Grupo Consolidado E21: Química Inorgánica y de los Compuestos Organometálicos). We also thank the “Generalitat Valenciana” for a fellowship (S.S.). The authors are grateful to the “Serveis Centrals d’Instrumentació Científica (SCIC)” of the Universitat Jaume I and the Instituto

de Biocomputación y Física de Sistemas Complejos (BIFI) and the Centro de Supercomputación de Galicia (CESGA) for generous allocation of computational resources.

## ■ REFERENCES

- (1) (a) Clapham, S. E.; Hadzovic, A.; Morris, R. H. *Coord. Chem. Rev.* **2004**, *248*, 2201–2237. (b) Gladiali, S.; Alberico, E. *Chem. Soc. Rev.* **2006**, *35*, 226–236. (c) Samec, J. S. M.; Bäckvall, J. E.; Andersson, P. G.; Brandt, P. *Chem. Soc. Rev.* **2006**, *35*, 237–248. (d) Palmer, M. J.; Wills, M. *Tetrahedron: Asymmetry* **1999**, *10*, 2045–2061. (e) Ikariya, T.; Blacker, A. J. *Acc. Chem. Res.* **2007**, *40*, 1300–1308. (f) Shimizu, H.; Nagasaki, I.; Matsumura, K.; Sayo, N.; Saito, T. *Acc. Chem. Res.* **2007**, *40*, 1385–1393.
- (2) (a) Noyori, R. *Adv. Synth. Catal.* **2003**, *345*, 15–32. (b) Noyori, R.; Ohkuma, T. *Angew. Chem., Int. Ed.* **2001**, *40*, 40–73. (c) Noyori, R.; Yamakawa, M.; Hashiguchi, S. *J. Org. Chem.* **2001**, *66*, 7931–7944. (d) Ohkuma, T.; Ooka, H.; Ikariya, T.; Noyori, R. *J. Am. Chem. Soc.* **1995**, *117*, 10417–10418. (e) Noyori, R. *Asymmetric Catalysis in Organic Synthesis*; Wiley: New York, 1994. (f) Hashiguchi, S.; Fujii, A.; Takehara, J.; Ikariya, T.; Noyori, R. *J. Am. Chem. Soc.* **1995**, *117*, 7562–7563. (g) Fujii, A.; Hashiguchi, S.; Uematsu, N.; Ikariya, T.; Noyori, R. *J. Am. Chem. Soc.* **1996**, *118*, 2521–2522. (h) Gao, J. X.; Ikariya, T.; Noyori, R. *Organometallics* **1996**, *15*, 1087–1089. (i) Takehara, J.; Hashiguchi, S.; Fujii, A.; Inoue, S.; Ikariya, T.; Noyori, R. *Chem. Commun.* **1996**, 233–234. (j) Uematsu, N.; Fujii, A.; Hashiguchi, S.; Ikariya, T.; Noyori, R. *J. Am. Chem. Soc.* **1996**, *118*, 4916–4917. (k) Haack, K. J.; Hashiguchi, S.; Fujii, A.; Ikariya, T.; Noyori, R. *Angew. Chem., Int. Ed.* **1997**, *36*, 285–288. (l) Matsumura, K.; Hashiguchi, S.; Ikariya, T.; Noyori, R. *J. Am. Chem. Soc.* **1997**, *119*, 8738–8739. (m) Noyori, R.; Hashiguchi, S. *Acc. Chem. Res.* **1997**, *30*, 97–102.
- (3) Zhao, B.; Han, Z.; Ding, K. *Angew. Chem., Int. Ed.* **2013**, *52*, 4744–4788.
- (4) Ikariya, T. In *Bifunctional Molecular Catalysis*; Ikariya, T., Shibasaki, M., Eds.; Springer: Berlin, 2011; Topics in Organometallic Chemistry Vol. 37, pp 31–53.
- (5) Degraauw, C. F.; Peters, J. A.; Vanbekkum, H.; Huskens, J. *Synthesis* **1994**, 1007–1017.
- (6) (a) Pàmies, O.; Bäckvall, J. E. *Chem. Eur. J.* **2001**, *7*, 5052–5058. (b) Bäckvall, J. E. *J. Organomet. Chem.* **2002**, *652*, 105–111.
- (7) (a) Baratta, W.; Chelucci, G.; Herdtweck, E.; Magnolia, S.; Siega, K.; Rigo, P. *Angew. Chem., Int. Ed.* **2007**, *46*, 7651–7654. (b) O, W. W. N.; Lough, A. J.; Morris, R. H. *Organometallics* **2012**, *31*, 2137–2151. (c) Ohara, H.; O, W. W. N.; Lough, A. J.; Morris, R. H. *Dalton Trans.* **2012**, *41*, 8797–8808.
- (8) (a) Mashima, K.; Abe, T.; Tani, K. *Chem. Lett.* **1998**, 1199–1200. (b) Murata, K.; Ikariya, T. *J. Org. Chem.* **1999**, *64*, 2186–2187. (c) Annen, S.; Zweifel, T.; Ricatto, F.; Gruetzmacher, H. *ChemCatChem* **2010**, *2*, 1286–1295. (d) Trincado, M.; Kuehlein, K.; Gruetzmacher, H. *Chem.—Eur. J.* **2011**, *17*, 11905–11913. (e) Annen, S. P.; Gruetzmacher, H. *Dalton Trans.* **2012**, *41*, 14137–14145. (f) Lang, F.; Breher, F.; Stein, D.; Gruetzmacher, H. *Organometallics* **2005**, *24*, 2997–3007. (g) Nova, A.; Taylor, D. J.; Blacker, A. J.; Duckett, S. B.; Perutz, R. N.; Eisenstein, O. *Organometallics* **2014**, *33*, 3433–3442.
- (9) (a) Bianchini, C. In *Iridium Complexes in Organic Synthesis*; Oro, L. A., Claver, C., Eds.; Wiley-VCH: Weinheim, Germany, 2008. (b) Fujita, K.; Yamaguchi, R. In *Iridium Complexes in Organic Synthesis*; Oro, L. A., Claver, C., Eds.; Wiley-VCH: Weinheim, Germany, 2008. (c) O, W. W. N.; Lough, A. J.; Morris, R. H. *Organometallics* **2013**, *32*, 3808–3818. (d) Dobereiner, G. E.; Nova, A.; Schley, N. D.; Hazari, N.; Miller, S. J.; Eisenstein, O.; Crabtree, R. H. *J. Am. Chem. Soc.* **2011**, *133*, 7547–7562. (e) Gnanamgari, D.; Sauer, E. L. O.; Schley, N. D.; Butler, C.; Incarvito, C. D.; Crabtree, R. H. *Organometallics* **2009**, *28*, 321–325. (f) Gnanamgari, D.; Moores, A.; Rajaseelan, E.; Crabtree, R. H. *Organometallics* **2007**, *26*, 1226–1230. (g) Chianese, A. R.; Crabtree, R. H. *Organometallics* **2005**, *24*, 4432–4436.

- (10) (a) Hintermair, U.; Campos, J.; Brewster, T. P.; Pratt, L. M.; Schley, N. D.; Crabtree, R. H. *ACS Catal.* **2014**, *4*, 99–108. (b) Campos, J.; Hintermair, U.; Brewster, T. P.; Takase, M. K.; Crabtree, R. H. *ACS Catal.* **2014**, *4*, 973–985. (c) Schley, N. D.; Halbert, S.; Raynaud, C.; Eisenstein, O.; Crabtree, R. H. *Inorg. Chem.* **2012**, *51*, 12313–12323. (d) Eisenstein, O.; Crabtree, R. H. *New J. Chem.* **2013**, *37*, 21–27.
- (11) Berliner, M. A.; Dubant, S. P. A.; Makowski, T.; Ng, K.; Sitter, B.; Wager, C.; Zhang, Y. *Org. Process Res. Dev.* **2011**, *15*, 1052–1062.
- (12) (a) Arita, S.; Koike, T.; Kayaki, Y.; Ikariya, T. *Organometallics* **2008**, *27*, 2795–2802. (b) Arita, S.; Koike, T.; Kayaki, Y.; Ikariya, T. *Chem. Asian J.* **2008**, *3*, 1479–1485. (c) Watanabe, M.; Kashiwame, Y.; Kuwata, S.; Ikariya, T. *Eur. J. Inorg. Chem.* **2012**, 504–511. (d) Sato, Y.; Kayaki, Y.; Ikariya, T. *Chem. Commun.* **2012**, *48*, 3635–3637. (e) Kashiwame, Y.; Kuwata, S.; Ikariya, T. *Organometallics* **2012**, *31*, 8444–8455.
- (13) (a) Barloy, L.; Issenhuth, J.-T.; Weaver, M. G.; Pannetier, N.; Sirlin, C.; Pfeffer, M. *Organometallics* **2011**, *30*, 1168–1174. (b) Jerphagnon, T.; Haak, R.; Berthiol, F.; Gayet, A. J. A.; Ritleng, V.; Holuigue, A.; Pannetier, N.; Pfeffer, M.; Voelklin, A.; Lefort, L.; Verzijl, G.; Tarabiono, C.; Janssen, D. B.; Minnaard, A. J.; Feringa, B. L.; de Vries, J. G. *Top. Catal.* **2010**, *53*, 1002–1008. (c) Pannetier, N.; Sortais, J.-B.; Issenhuth, J.-T.; Barloy, L.; Sirlin, C.; Holuigue, A.; Lefort, L.; Panella, L.; de Vries, J. G.; Pfeffer, M. *Adv. Synth. Catal.* **2011**, *353*, 2844–2852. (d) Sortais, J.-B.; Pannetier, N.; Clement, N.; Barloy, L.; Sirlin, C.; Pfeffer, M.; Kyritsakas, N. *Organometallics* **2007**, *26*, 1868–1874.
- (14) Cross, W. B.; Daly, C. G.; Boutadla, Y.; Singh, K. *Dalton Trans.* **2011**, *40*, 9722–9730.
- (15) Davies, D. L.; Al-Duaij, O.; Fawcett, J.; Giardiello, M.; Hilton, S. T.; Russell, D. R. *Dalton Trans.* **2003**, 4132–4138.
- (16) (a) Cahn, R. S.; Ingold, C.; Prelog, V. *Angew. Chem., Int. Ed.* **1966**, *5*, 385–&. (b) Brunner, H. *Enantiomer* **1997**, *2*, 133–134.
- (17) (a) Sabater, S.; Mata, J. A.; Peris, E. *Organometallics* **2013**, *32*, 1112–1120. (b) Hockless, D. C. R.; Gugger, P. A.; Leung, P. H.; Mayadunne, R. C.; Pabel, M.; Wild, S. B. *Tetrahedron* **1997**, *53*, 4083–4094.
- (18) (a) Comas-Vives, A.; Ujaque, G.; Lledós, A. *Organometallics* **2007**, *26*, 4135–4144. (b) Dub, P. A.; Ikariya, T. *J. Am. Chem. Soc.* **2013**, *135*, 2604–2619.
- (19) (a) Comas-Vives, A.; Ujaque, G.; Lledós, A. *J. Mol. Struct. (THEOCHEM)* **2009**, *903*, 123–132. (b) Comas-Vives, A.; Ujaque, G.; Lledós, A. In *Theoretical and Computational Inorganic Chemistry*; Van Eldik, R., Harvey, J., Eds.; Elsevier: Amsterdam, 2010; Advances in Inorganic Chemistry Vol. 62, pp 231–260. (c) Alonso, D. A.; Brandt, P.; Nordin, S. J. M.; Andersson, P. G. *J. Am. Chem. Soc.* **1999**, *121*, 9580–9588. (d) Di Tommaso, D.; French, S. A.; Zanotti-Gerosa, A.; Hancock, F.; Palin, E. J.; Catlow, C. R. A. *Inorg. Chem.* **2008**, *47*, 2674–2687. (e) Nieto Faza, O.; Fernandez, I.; Silva Lopez, C. *Chem. Commun.* **2013**, *49*, 4277–4279. (f) Petra, D. G. I.; Reek, J. N. H.; Handgraaf, J. W.; Meijer, E. J.; Dierkes, P.; Kamer, P. C. J.; Brussee, J.; Schoemaker, H. E.; van Leeuwen, P. *Chem. Eur. J.* **2000**, *6*, 2818–2829. (g) Zhang, X.; Guo, X.; Chen, Y.; Tang, Y.; Lei, M.; Fang, W. *Phys. Chem. Chem. Phys.* **2012**, *14*, 6003–6012.
- (20) (a) Bi, S.; Xie, Q.; Zhao, X.; Zhao, Y.; Kong, X. *J. Organomet. Chem.* **2008**, *693*, 633–638. (b) Handgraaf, J. W.; Reek, J. N. H.; Meijer, E. J. *Organometallics* **2003**, *22*, 3150–3157.
- (21) W. N. O, W.; Lough, A. J.; Morris, R. H. *Organometallics* **2012**, *31*, 2152–2165.
- (22) (a) Gridnev, I. D.; Watanabe, M.; Wang, H.; Ikariya, T. *J. Am. Chem. Soc.* **2010**, *132*, 16637–16650. (b) Chen, L.-A.; Xu, W.; Huang, B.; Ma, J.; Wang, L.; Xi, J.; Harms, K.; Gong, L.; Meggers, E. *J. Am. Chem. Soc.* **2013**, *135*, 10598–10601. (c) Hounjet, L. J.; Ferguson, M. J.; Cowie, M. *Organometallics* **2011**, *30*, 4108–4114.
- (23) Clark, R. C.; Reid, J. S. *Acta Crystallogr., Sect. A* **1995**, *51*, 887–897.
- (24) (a) Sheldrick, G. M. *Acta Crystallogr., Sect. A* **2008**, *64*, 112–122. (b) Dolomanov, O. V.; Bourhis, L. J.; Gildea, R. J.; Howard, J. A. K.; Puschmann, H. *J. Appl. Crystallogr.* **2009**, *42*, 339–341.
- (25) Frisch, M. J., et al. *Gaussian 09, revision D.02*; Gaussian, Inc., Wallingford, CT, 2009.
- (26) Zhao, Y.; Truhlar, D. G. *Theor. Chem. Acc.* **2008**, *120*, 215–241.
- (27) Andrae, D.; Häussermann, U.; Dolg, M.; Stoll, H.; Preuss, H. *Theor. Chim. Acta* **1990**, *77*, 123–141.
- (28) Ehlers, A. W.; Böhme, M.; Dapprich, S.; Gobbi, A.; Höllwarth, A.; Jonas, V.; Köhler, K. F.; Stegmann, R.; Veldkamp, A.; Frenking, G. *Chem. Phys. Lett.* **1993**, *208*, 111–114.
- (29) Harihara, P. C.; Pople, J. A. *Theor. Chim. Acta* **1973**, *28*, 213–222.
- (30) Francl, M. M.; Pietro, W. J.; Hehre, W. J.; Binkley, J. S.; Gordon, M. S.; Defrees, D. J.; Pople, J. A. *J. Chem. Phys.* **1982**, *77*, 3654–3665.
- (31) Marenich, A. V.; Cramer, C. J.; Truhlar, D. G. *J. Phys. Chem. B* **2009**, *113*, 6378–6396.